Article:

Gao, J, Guo, H, Wang, X et al. (5 more authors) (2019) Microwave deicing for asphalt mixture containing steel wool fibers. Journal of Cleaner Production, 206. pp. 1110-1122. ISSN 0959-6526

https://doi.org/10.1016/j.jclepro.2018.09.223

Accepted Manuscript

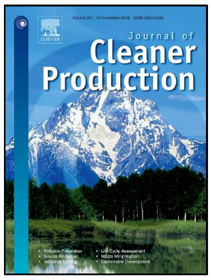

Microwave deicing for asphalt mixture containing steel wool fibers

Jie Gao, Haoyan Guo, Xiaofeng Wang, Pei Wang, Yongfeng Wei, Zhenjun Wang, Yue Huang, Bo Yang

PII: S0959-6526(18)32956-1

DOI: 10.1016/j.jclepro.2018.09.223

Reference: JCLP 14358

To appear in: *Journal of Cleaner Production*

Received Date: 15 May 2018

Accepted Date: 25 September 2018

Please cite this article as: Jie Gao, Haoyan Guo, Xiaofeng Wang, Pei Wang, Yongfeng Wei, Zhenjun Wang, Yue Huang, Bo Yang, Microwave deicing for asphalt mixture containing steel wool fibers, *Journal of Cleaner Production* (2018), doi: 10.1016/j.jclepro.2018.09.223

Microwave deicing for asphalt mixture containing steel wool fibers

Jie Gao[1, 3], Haoyan Guo[2], Xiaofeng Wang[4], Pei Wang[2], Yongfeng Wei[5], Zhenjun Wang[2*], Yue Huang[6], Bo Yang[4]

1. School of Highway, Chang'an University, Xi'an 710064, China;

2. School of Materials Science and Engineering, Chang'an University, Xi'an 710061, China.

3. Department of Civil Engineering, Liverpool John Moores University, Peter Jost Enterprise Centre, Byrom Street, L3 3AF Liverpool, United Kingdom

4. Henan Provincial Communications Planning & Design Institute Co., Ltd., Zhengzhou 450052, P.R. China;

5. Pavement Engineering Technology Center, Gansu Road and Bridge Construction Group Co., Ltd. Lanzhou 730030, China;

6. Institute for Transport Studies, University of Leeds, Leeds LS2 9JT, United Kingdom

*Corresponding author: Zhenjun Wang, Ph.D., Professor; E-mail: wangzhenjun029@163.com

Abstract: Driving safety deteriorated dramatically on ice-covered road pavement in winter. However, it is a challenge to remove thick ice layer from the pavement surface with conventional technologies. In this study, the microwave heating performance of asphalt mixtures containing steel wool fibers was tested. Firstly, the mechanism of pavement deicing using microwave was introduced. The effect of steel wool fiber on air void content of asphalt mixture is studied, and the fiber distribution is observed. The microwave heating performance of specimens with different types and contents of steel wool were tested under the temperature of -5 °C and -10 °C. The ice-thawing time was measured and the effect of initial temperature and ice thickness on the thawing time was evaluated. Finally, the heating uniformity and sustainability aspects of this technique were assessed. Results show that the optimal steel wool fiber contents for microwave heating of asphalt mixture are 0.3% of 000#, 0.6% of 0# and 0.9%% of 2#, respectively. The ice-thawing time of the pavement with an initial temperature of -10 °C is 9.3% (000#), 11.3% (0#) and 14.8% (2#) higher than that of -5 °C. In addition, every 1cm increase in ice layer thickness requires 5.9% (000#), 7.7% (0#) and 13.0% (2#) increase in thawing time. A larger diameter of the steel wool helps to improve the heating uniformity. At last, the microwave heating capacity of specimens containing steel wool will not be significantly reduced by the repeated service in the first five winters.

Key words: microwave deicing, asphalt pavement, steel wool, ice-thawing

1. Introduction

Driving safety deteriorated dramatically in winter resulting from the snowfall or ice accumulated on the pavement, leading to a significant reduction in pavement-tire friction and increasing the risk of accidents. Transportation researchers have made great efforts to demonstrate that the icy road is responsible for a number of driving injuries or fatalities, traffic delays and economic losses (Bardal and Jørgensen, 2017; Khaleghei Ghosheh Balagh et al., 2014; Strong et al., 2010; Theofilatos, 2017) .

Nowadays, a lot of road snow and ice control technologies have been developed which are associated with advanced materials, new products, machines, maintenance strategies and operations. For instance, the deicer chemicals or the anti-freeze filler contained in the asphalt concrete, are effective in preventing the icy condition (Liu et al., 2016), however, the chlorides contained in these chemicals have been blamed for having a damaging effect on the aquatic ecology, flora and fauna and, in addition, are considered corrosive to the pavement materials (Rivett et al., 2016; Wyman and Koretsky, 2018; Zítková et al., 2018). The heat melting method adopts special facilities to collect, store, transform and release external energy to generate heat for melting snow or ice on the road surface (Pan et al., 2015; Zhang et al., 2016; Zhou et al., 2015). The external energy, for example, geothermal or solar, are environment friendly and renewable energy resources for humans, while the equipment using conventional energy (e.g. natural gas and electric energy) may strain the city's energy supply system. Generally, conventional heat melting methods result in high construction investment and operating expenses.

Microwave heating (MH) has attracted great interest from the industry and academia thanks to its advantages of high uniformity, energy saving, selective heating and environmental friendliness; the method has seen numerous applications in many industrial processes (Tang et al., 2018). Early researchers tried to introduce the MH technology into pavement ice-melting. These efforts however, have not yielded the satisfactory results due to the fact that conventional road materials such as the asphalt, cement and aggregate have limited MH capacity (Osborne and

Hutcheson, 1987). Therefore, various microwave absorbing materials were utilized for surface layer of the pavement to enhance the MH capacity of conventional pavement. For instance, Hopstock and Zanko (2005) used taconite produced in Minnesota as the aggregate for preparation of the asphalt mixtures, the laboratory tests showed that the heat capacity, thermal conductivity and microwave absorption of taconite asphalt mixtures were greatly improved. In addition, Jahanbakhsh et al. (2018) and Karimi et al. (2018) reported that conductive admixtures such as carbon fiber and carbon black are effective for enhancing the microwave heating rate of asphalt mixture, and they also indicated that the limestone aggregate is better than the siliceous aggregate concerning the microwave heating rate. Furthermore, Wang' group (Gao et al., 2017; Wang et al., 2014; Wang, Z. et al., 2016a; Wang, Z. et al., 2016b; Wang, Z. et al., 2016c) has made great efforts in incorporating microwave absorbing materials to conventional asphalt pavement.

Although a number of options are now available for improving the electromagnetic properties of asphalt mixtures, the development of MH ice-melting techniques for asphalt mixture containing steel wool or steel fiber has concentrated insufficient attention (Gao et al., 2016). The utilization of steel fiber - reinforced asphalt concrete (SFRAC) in surface layer for pavement has been proven to be an effective way to improve pavement mechanical and fatigue properties. For instance, Wang (Wang, H. et al., 2016) reported that the asphalt concrete containing an optimal amount (0.4 wt%, 0.1 mm diameter) of steel fibers has seen significant improvement in Marshall stability, rutting resistance, indirect tensile strength, and low temperature cracking resistance compared to conventional asphalt concrete. Park' research (Park et al., 2015) demonstrated that the low temperature cracking resistance of asphalt concrete can be significantly improved by adding the steel fibers with 0.5-1.5 vol% content, 0.1-0.4 mm diameter and 6-30 mm length. Similar conclusions are also found in He's research (He et al., 2017). Furthermore, the steel wool fiber, which is known as the steel fiber with finer diameter, is reported advantageous for improving the particle loss resistance and flexural strength of dense asphalt concrete. However, the steel wool fibers tend to be clustered as compared to the steel fiber, the aggregate gradation and bitumen percentage in the mixture should be adjusted to avoid high air voids caused by the fiber clusters (García et al., 2013). The recommendations made by García is to use the shorter steel wool fiber with the larger diameter. In the meantime, the electromagnetic heating characteristics of SFRAC have also been explored in previous studies. For example, Garcia' group (García et al., 2013; García et al., 2012; García et al., 2010; Menozzi et al., 2015; Norambuena-Contreras and Garcia, 2016; Obaidi et al., 2017) have carried out intensive studies to introduce the self-healing performance of asphalt concrete with steel wool using the electromagnetic induction heating technology. Results show that the surface temperature of asphalt concrete with more than 4% (by volume of binder) steel wool fiber can be heated up to 60 °C after 120s electromagnetic wave irradiation (6 kW, 350 kHz). However, the modified mixture with 2%, 4%, 6% and 8% fiber content lead respectively to 7.92%, 8.67%, 8.96% and 10.54% air voids content. Compared to the reference mixture (air voids content was 5.98%), higher air voids is responsible for exponentially increasing of the particle loss of dense asphalt concrete (García et al., 2013; Norambuena-Contreras and Garcia, 2016). Meanwhile, Liu's researches (Liu et al., 2010; Liu et al., 2013; Liu et al., 2014) obtained similar conclusions concerning the heating properties.

These preliminary findings justified the need to conduct a primary study to verify the feasibility of MH deicing for asphalt pavement surface layer containing steel wool. Objectives of this study will be to:

- Recommend the optimal steel wool content with various diameters for pavement microwave deicing;
- and investigate the microwave deicing efficiency of asphalt mixtures containing steel wool under various operating conditions.

In this study, the surface temperature of asphalt mixtures containing various types and contents of steel wool after microwave irradiation under different initial temperatures was assessed via laboratory research to determine the optimal usage. The effect of initial pavement temperature and ice layer thickness on the ice-thawing times of asphalt mixtures with steel wool was investigated. At last, the heating uniformity and the sustainability constraints of heating capacity were analyzed to overcome the potential barriers that may be encountered in practice. The materials developed in this study offer a novel technical solution to the removal of thick ice on winter pavement, especially for critical locations such as airport runway, bridge deck and sharp bend.

2. Method

2.1 Materials

The aggregate was limestone produced in Shaanxi province, China, with an apparent specific gravity 2.772 g/cm^3, soaking swelling ratio 0.4%, water absorption 0.71% and crushing value 20.4%, which meet the Chinese specification for the Testing Procedures of Aggregate for Highway Engineering in China (JTG E42- 2005) (JTGE42-2005, 2005). The mineral compositions of aggregate obtained by X-Ray diffraction are shown in Fig. 1.

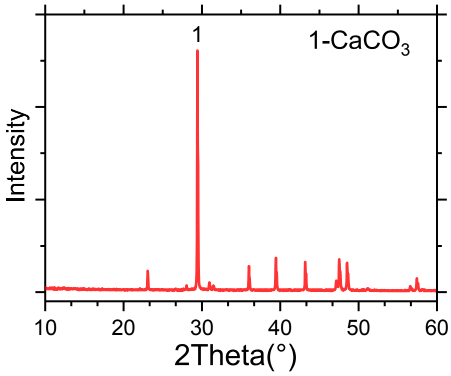

Fig.1 X-Ray diffraction results of limestone aggregate

Binder was the base bitumen with a density of 1329 kg/m^3 produced in Kuwait, its properties are shown in Table 1. In addition, three types of low-carbon steel wool (000#, 0# and 2#) with different diameters were used for the preparation of the asphalt mixtures. The crude steel wool fiber was processed into shorter products by a wheel cutter. The steel type was S434 stainless steel, its chemical composition can be found in Table 2. Approximately 90 fibers for each steel wool type were selected randomly, then the length distribution of three steel wool types were investigated jointly using optical microscope and image processing software. The technical parameters, topography and length distribution of the used steel wool fiber is summarized in Table 2.

Table 1 Properties of asphalt binder

Properties	Unit	Specification	Test results
Penetration (25°C, 5s, 100g)	0.1mm	60~80	72
Softening point R&B (R&B method)	^{o}C	≥46	52.3
15 ^{o}C ductility	cm	≥40	51
Solubility	%	≥99.5	99.71
15 ^{o}C density	g/cm^3	Measured	1.329
Wax content (distillation method)	%	≤2.2	1.7
Flash Point (COC)	^{o}C	≥260	305

Table 2 Technical parameters and length distribution of steel wool fiber

Types	Diameter	Electrical	Density	Length distribution / mm

	(μm)	resistivity (Ωcm)	(g/cm^3)	<5	5-6	6-7	7-8	8-9
000#	15 - 35	7×10^{-7}	7.72	12%	6%	43%	27%	12%
0#	50 - 70			5%	11%	44%	32%	8%
2#	75 - 125			7%	4%	49%	29%	11%
Steel	Chemical Composition/%							
434 stainless steel	C	Mn	Si	Cr	P	S	Mo	
	≤0.12	≤1.00	≤1.00	16.0-18.0	≤0.04	≤0.03	0.75-1.25	
Topography								

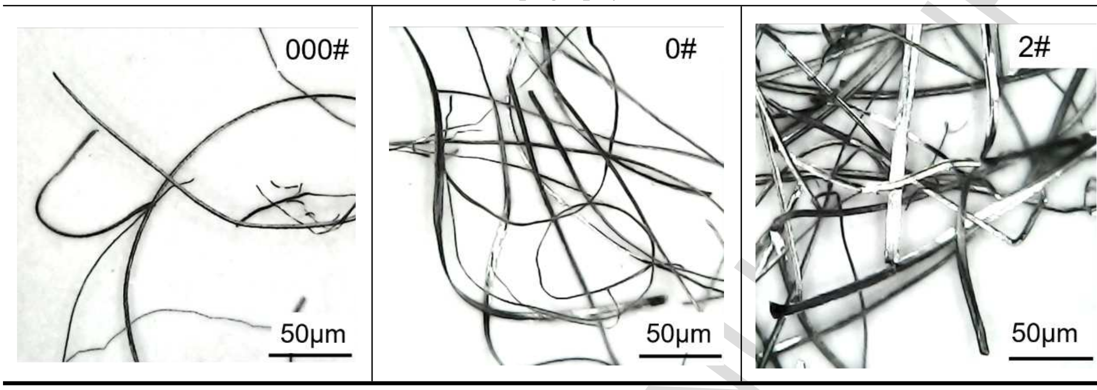

2.2 Tests

2.2.1 Preparation of the specimens

The mid-value of the dense AC-13 aggregate gradation recommended in Chinese Technical Specification for Construction of Highway Asphalt Pavement (JTG F40-2004) (JTGF40-2004, 2004) was used to prepare the specimens for Marshall test, as shown in Table 3. The optimal asphalt binder content was 5.5%, which was obtained from the Marshall tests for the specimens without steel wool fiber. The content of different steel wool types used in specimens was determined by observation of the steel wool fiber aggregation level during the mixing process of the asphalt mixtures. For example, Fig.2 presents the fact that the steel wool fiber clusters were formed during the mixing process of asphalt mixtures containing 0.6% (by volume) of 000# steel wool, the diameter of steel wool fiber clusters was in range of 1 - 3 cm. Similarly, the saturation (when the steel wool clumps become visible) content of steel wool 0# and 2# in specimens were evaluated. Based on the observations, the steel wool fiber contents by volume in specimens are designed to be: 0.1% - 0.4% for 000# type, 0.1% - 0.9% for 0# type and 0.1% - 1.3% for 2# type, with 0.1% interval. Three specimens were prepared for each steel wool fiber content via Marshall Compaction.

Table 3 Aggregate gradation for Marshall specimens

	Sieve size/mm										
	Filler	0.075	0.15	0.3	0.6	1.18	2.36	4.75	9.5	13	16
Aggregate mass retained/%	6	4	3.5	5.5	7.5	10.5	16	23.5	18.5	5	0
Mass/g	71	47	41	65	89	124	190	279	219	59	0

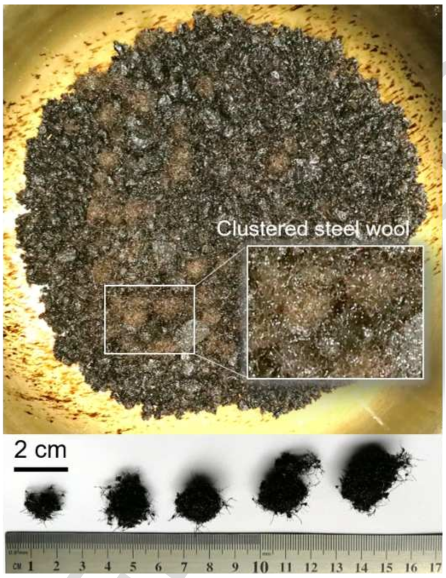

Fig.2 Outlook of the asphalt mixture with 0.6% of 000# steel wool fiber

2.2.2 Air void content and fiber distribution

The air void content of asphalt mixture prepared with various steel wool fibers are tested in accordance with the Chinese specification (JTGF40-2004, 2004). In addition, to investigate the steel wool fiber distribution in the asphalt mixture, the Marshall specimens containing various steel wool fiber contents and fiber types are prepared, and each specimen is cut open. The photos of the fracture surface for each specimen are captured by using a CCD camera.

2.2.3 Surface temperature test

The surface temperature of specimens after microwave heating were recoded by using a mearing system, as illustrated in Fig.3 (a), it consists of a voltage stabilizer, a mini-scale microwave unit and an infrared camera. Generally, the microwave unit installed on the MH vehicle is designed with approximately 80 - 120 magnetrons, thus it can heat a large area. For laboratory study, a mini-scale microwave unit was developed to simulate the field working process of the MH vehicle (as shown in Fig.3 (b)), the magnetron had a 2.45GHz frequency and 800W power output. Furthermore, the magnetron was embedded in a metal device to prevent microwave leakage and the ventilating fan was designed to dissipate possible smoke. The voltage stabilizer was purpose-designed to maintain a stable power supply and to transmit the power from the power generator in field working, its technical parameters are input range 105V - 450V and output 220V±4%. In addition, the thermal images were captured by a CS320 infrared camera whose performance parameters are 100 × 80 pixels infrared resolution, -30 °C ~ 200 °C test range, ±2 °C error range, 0.08 °C temperature sensitivity. The Marshall specimens containing steel wool were embedded in an asphalt concrete slab, as shown in Fig.3 (c). During the heating, the thermal images of the specimens' surface were captured every 20 seconds after removing the microwave unit from the slab. The temperature matrix of the area captured in thermal images can be observed, stored and extracted via the built-in software, the average temperature and standard deviation can be calculated based on the data matrix.

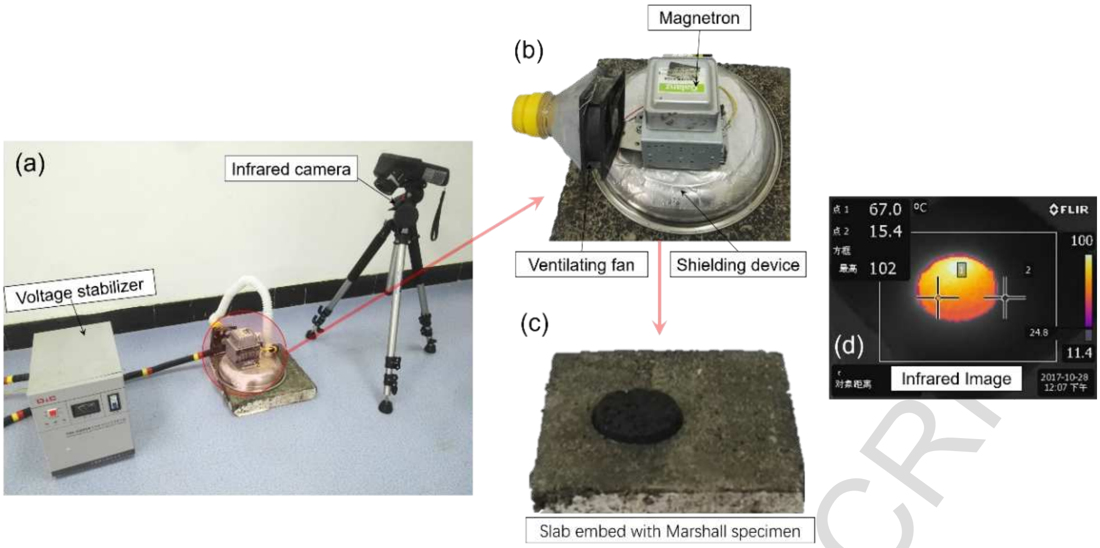

(a) measuring system for pavement MH surface temperature; (b) mini-scale microwave unit; (c) asphalt concrete embedded with the Marshall specimen; (d) typical thermal image

Fig.3 Setup for temperature test

2.2.4 Ice-thawing time test

To simulate the condition of ice layer covered on the road surface in winter, especially under extremely unfavorable conditions (e.g. freezing rain, frozen residual rainwater and compacted snow), three thicknesses of ice were designed as 3cm, 4cm and 5cm. A plastic collar with a scale (in cm) was hoop strapped on the Marshall specimen via a liner and a belt. The ice layer can be created after the specimens were placed in a freezer and tap water injected in the collar. The designed thickness, can be realized by control the water injection volume. The setup for ice layer preparation and the outlook of the prepared ice layer are demonstrated in Fig. 4 (a) and (b), respectively.

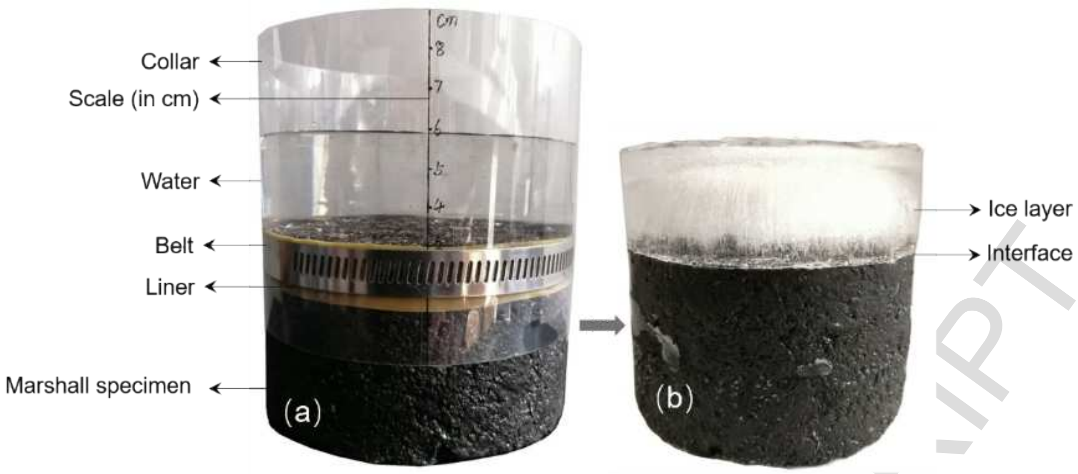

(a) setup; (b) prepared ice layer

Fig. 4 Ice layer preparation

The accelerated MH de-icing device was designed to test the ice-thawing time required for the MH vehicle in field working process. In practice, the ice layer will be shoveled out after the pavement have been heated by microwave irradiation. The horizontal force applied by the shovel to overcome the adhesion between ice layer and pavement f_{hc} was simulated by the accelerated MH de-icing device, the f_{hc} value was referenced to previous study which can be calculated using Eq. (1) (Sun, 2013). In this case, 3.95 N, 5.26 N and 6.58 N were used for 3 cm, 4 cm and 5cm thick ice layers, respectively.

$$f_{hc} = \frac{\int_0^{2r} 2h\rho_x v^2(1+0.73\sin^2\theta - 0.33\cos^2\theta)\sqrt{r^2-(r-x)^2}dx}{2r} - \pi r^2 h\rho g \quad \text{Eq. (1)}$$

Where, r is the radius of the Marshall specimen, m; h is the thickness of ice layer, m; ρ is the density of the ice, kg/m^3; v is the speed that MH vehicle is operating, km/h; θ is the angle between the road and shovel, °; x is the distance between the integration point and the surface edge, m.

The f_{hc} was applied and adjusted by varying the stretch height of the rubber band with a spring dynamometer. The stretch height can be consistent for specimens via a fixed point, as shown in Fig. 5 (a). During the ice-thawing test, the specimen was placed into a microwave oven along with the accelerated MH de-icing device. The magnetron in microwave oven has the same properties as those used in surface temperature test. The ice-thawing time was recorded when the ice layer was completely removed, as illustrated in Fig. 5 (b).

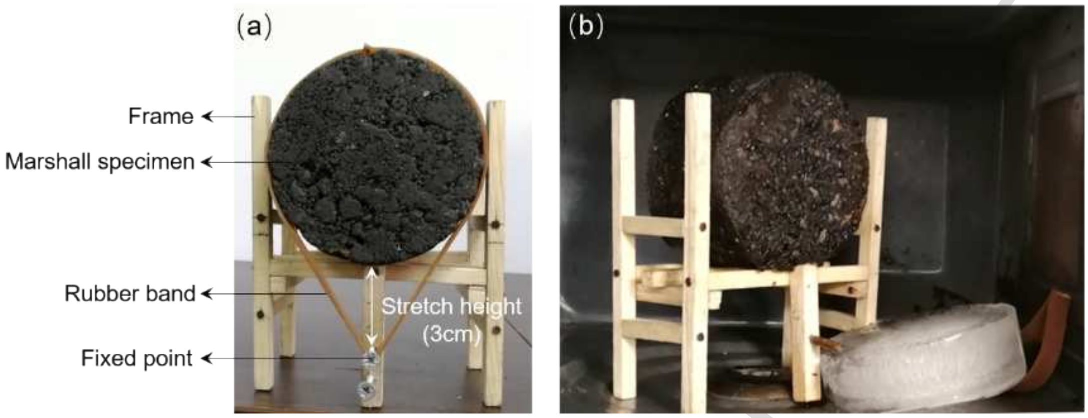

(a) setup; (b) removed ice layer

Fig. 5 Accelerated MH de-icing device

2.2.5 Heating durability

Freeze-thaw cycle was used to create the actual environment that the MH pavement experienced in the deicing process. The heating effect on the mixtures can be assessed by comparing the surface temperatures before and after freeze-thaw cycles. A complete freeze-thaw cycle consists of four steps which are (i) specimens were placed in room temperature (20 ± 2°C) for 160 min, (ii) they were soaked in water for 180 min, (iii) they were then frozen in a freezer at -10 °C for 120 min, and (iv) they were heated with microwave for 3 min.

3 Working mechanism of pavement microwave deicing technology

Microwave deicing pavement requires not only effective microwave-absorbing agents but also a purpose-designed operating machinery. The prototype of MH deicing vehicle was jointly designed by academic and industry in China on 2000, and the commercial model is now available in Chinese market (Jiao et al., 2008; Li et al., 2003; Yu et al., 2011). Fig. 6 demonstrates a typical outlook of the MH deicing vehicle which contains a series of core components such as crusher, shovel, magnetron matrix and generator unit. The magnetron matrix is the key module consisting of 70 - 120 magnetrons to create a heating wall with a typical heating area above 3 m^2.

A standard pavement MH deicing process usually consists of two steps. Firstly, the magnetron matrix converts electricity to electromagnetic energy and irradiates the pavement. The adhesion of freezing - thawing interface between asphalt concrete and ice layer barely remains after the microwave heating. However, a controlled microwave heating time is required in the first step because the insufficient heating time has limited effect on the interface melting while the excessive heating time leads to the refrozen of melted water under low-temperature atmosphere. In the second step, the ice layer will be pulverized by the crusher and pushed to the road-side by the shovel such that the ice layer can be removed easily.

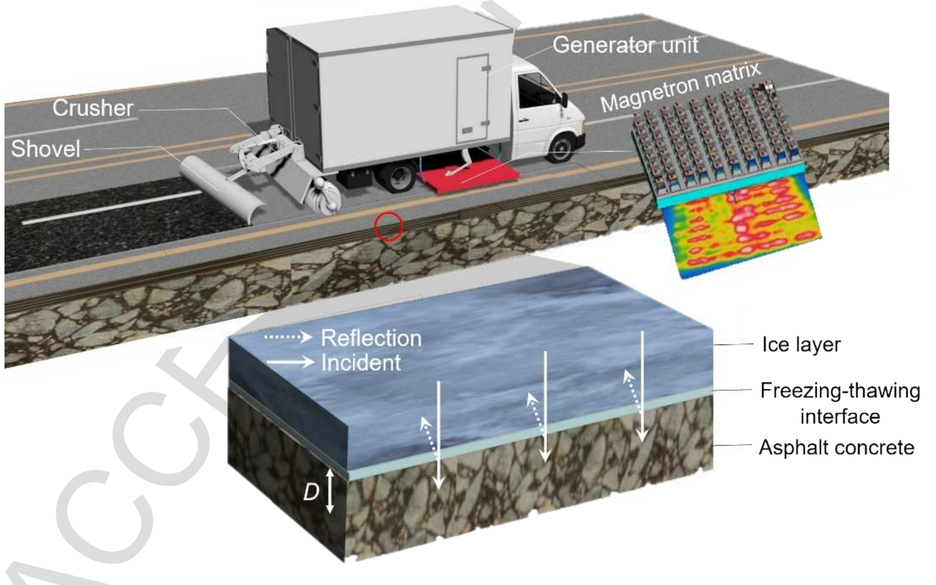

Fig.6 Prototype design for MH deicing vehicle

Basically, the MH deicing efficiency is influenced by the pavement material properties and MH vehicle design. When microwaves are applied to the pavement surface, part of the electromagnetic waves are reflected and lost while the remaining electromagnetic waves are absorbed by the pavement surface. The microwave power absorbed in unit volume of material can be calculated using Eq.2 (Tang, 2009). Generally, *tanδ* is the main indicator of the pavement's ability to absorb microwaves, which can be effectively improved by adding microwave absorbing materials. In fact, microwave is generally able to penetrate the pavement after the electromagnetic wave enters the pavement surface (10 – 12 cm), but the microwave power declines substantially along the vertical direction (Tang, 2009). For example, Jahanbakhsh et al. (2018) and Karimi et al. (2018) compared the microwave heating rate of asphalt mixture containing conductive materials under different thicknesses, the results show that the thinner specimens is of higher heating rate, namely the closer to the surface, the higher the temperature. The penetration depth of microwave into the pavement can be calculated using Eq. 3. Technically, a lower penetration depth with a higher energy density benefits the MH deicing as the transfer of heat is more efficient, while the problem of overheating the underlying asphalt mixture can be avoided. Apparently, Eq. 3 indicates that microwave penetration depth can be reduced by increasing the dielectric loss tangent and the relative permittivity of the asphalt mixture.

$$P = 0.556 f \varepsilon_r' \tan\delta \times E^2 \times 10^{-12} \qquad \text{Eq. (2)}$$

$$D = \frac{\alpha}{\pi\sqrt{2\varepsilon_r'\left\{\sqrt{1+\tan^2\delta}-1\right\}}} \qquad \text{Eq. (3)}$$

Where, P is microwave power absorbed in unit volume of material, W/cm^3; f is the frequency of microwave, Hz; $\tan\delta$ is dielectric loss tangent, no unit; ε_r' is relative permittivity of asphalt mixture, no unit; E is electric field strength, V/cm; D is penetration depth of the microwave into the pavement surface, cm;

As reported in previous studies, the desirable microwave heating efficiency required by MH vehicle is determined jointly by the distance between magnetron and pavement ($D_{M\text{-}P}$), the magnetron power and the frequency of electromagnetic waves (Sun, 2013; Tang, 2009). The 5.8 GHz microwave magnetron is reported to be 4 - 6 times more efficient than 2.54 GHz microwave magnetron in deicing pavement with the same power (Jiao et al., 2008). Studies also indicated that a higher frequency electromagnetic wave is preferred because it has lower heating depth (Sun et al., 2018). Tang (2009) pointed out the heating rate of a magnetron with 1700 W power is 1.8 times higher that of 1000 W power. Jiao' study (Gao et al., 2009) indicated that the maximum power density of asphalt concrete decreases by 72% when the $D_{M\text{-}P}$ increases from 10 mm to 100 mm, indicating the higher $D_{M\text{-}P}$, the lower MH efficiency.

4 Results and discussions

4.1 Air void and fiber distribution

4.1.1 Air void

The incorporation of steel wool fiber could change the volumetric properties of asphalt mixture, especially on the air void content, which is believed to be related with the durability of the asphalt mixture. Therefore, the effect of steel wool fiber on the air void content of asphalt mixture is investigated, and the results are shown in Fig. 7. According to Fig. 7, there are two primary effects can be observed. First, compared to the air void content of specimens without fibers (2.72%), the incorporation of steel wool fiber increases the air void of asphalt mixture regardless of the fiber contents and fiber types. Meanwhile, it can be observed that the increasing fiber contents lead to the higher air void contents regardless of the fiber types. Second, the asphalt mixtures with thinner fibers have higher air voids. The incorporation of the thinnest 000# fibers increases the air void contents of asphalt mixture form 2.72% to and 5.45% and 5.88% when fiber content is 0.2% and 0.4, respectively. On the other hand, when the 0# and 2# contents below 0.6%, the air void of the mixture is lower than that of the mixture with 0.4% of 000# fiber. Similarly, the 2# fiber leads to lower air void contents compared to that of 0# fiber at the same fiber content. In addition, it is clear that the air void of the mixture soaring greatly to 8.25% and 6.66% when 0.9% of 0# and 2# fibers are used, respectively; the air void content of the mixture increases to 9.22% after 1.2% of 2# fibers were used. As previous studies have pointed out that the higher air void could cause the deterioration of durability in terms of particle loss mass (García et al., 2013). From this view, it is not recommended to use more than 0.9% by volume of fibers in the asphalt mixture.

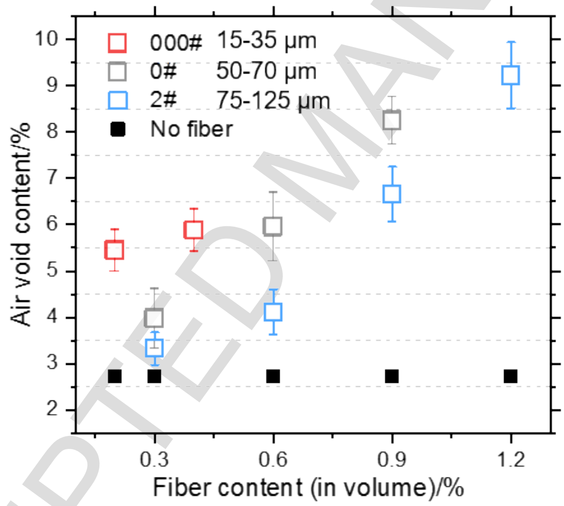

Fig. 7 Effect of steel wool fiber on the air void content of asphalt mixture

4.1.2 Fiber distribution

Fig. 8 demonstrates the steel wool fiber distribution in the asphalt mixtures with different fiber contents and fiber types. In Figure 8, the fiber distribution density can be divided into three grades, namely low density, high density and fiber clusters. Low density refers to the area where the fibers are separately distributed, and high density refers to the area where the fibers contact each other; the fiber cluster refers to the area where the fibers are intertwined with each other at a higher density. Based on the observation of Fig. 8, the first finding is that a higher fiber content leads to more intensive fiber clusters, this phenomenon that can be observed in all samples. For example, when 2# fiber is used, it is can be seen that the steel wool fibers are separately distributed, neither high-density area nor cluster are observed in the fracture surface of specimens until the fiber content exceeds 0.6%. Similarly, as the content of 000# and 0# fiber increases, the fiber cluster is getting more obvious. The second finding is that the thinner steel wool fiber is more easily to be clustered inside the asphalt mixture compared to the thicker fiber. This finding can be proven through the comparison between the fiber distribution of the 0# and 2# fiber. It is apparent that the incorporation of thinner 0# fibers results in larger and more clusters in the asphalt mixture at the same fiber content compared to the thicker 2# fibers.

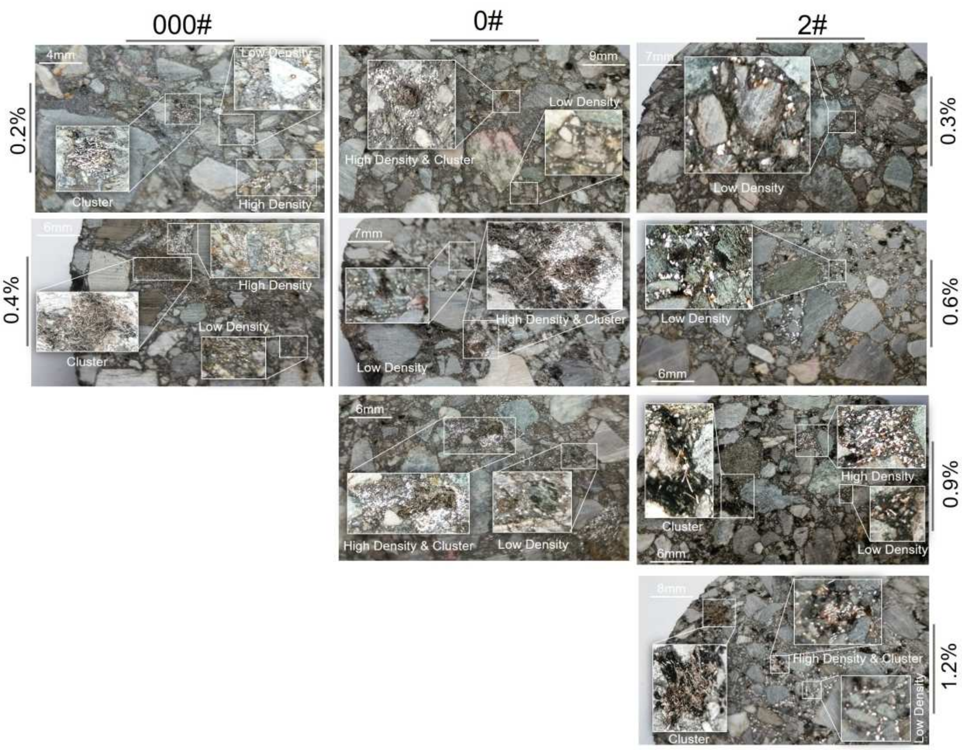

Fig. 8 Distribution of the steel wool fiber in asphalt mixture

4.2 Microwave heating performance

Generally, the primary barrier for using MH in deicing pavement in practice is the insufficient operating efficiency that hinders the MH vehicle running at a desirable operating speed. Therefore, the effect of steel wool on the MH performance of asphalt mixtures should be firstly evaluated. Fig.9 presents the surface temperature of asphalt mixtures containing three fiber types at various contents after different microwave irradiation durations (initial temperature was 18 °C). In Fig. 9, surface temperatures of the asphalt mixtures increase with the increase of the microwave irradiation time, this effect is clearly observed in all specimens regardless of steel wool contents and types. Obviously, the surface temperature increases after steel wool is added. The increases in surface temperature of specimens with 000#, 0# and 2# steel wool are 60-75ºC, 50-95ºC and 45-105ºC, respectively, higher than that of control asphalt mixture after the same irradiation time (180s). Furthermore, it shows that the surface temperature increases with the increase of the steel wool contents firstly and then decreases as the steel wool contents continue to increase. In Fig. 9(a), the surface temperature of 000# specimens increase from 24.8 °C (0%) to the highest point 97.4 °C (0.3%) and then drops to 89.8 °C (0.4%) after 180 s irradiation. Similarly, mixtures containing 0# steel wool have its surface temperature reach the maximum 122.1 °C with 0.6% of steel wool, then it declines to 114.8 °C when the steel wool content reaches 0.9%, as shown in Fig. 9(b). The specimens with 2# steel wool have high surface temperatures when the steel wool contents are 0.9% (127.8 °C), 1.0% (128.6 °C) and 1.1% (127.9 °C) and the temperature decreases to 114.0 °C with the highest steel wool content 1.3%, as shown in Fig. 9(c). It is clear that the content of steel wool fiber cluster increases when steel wool fiber content over a certain amount, the clusters cannot be microwave heated because they reflect electromagnetic waves. Therefore, the specimens see their surface temperatures decrease when the fiber contents exceed a certain amount resulting from the increasing clusters. As the results indicate, the optimal steel wool contents for asphalt mixtures having highest surface temperature after microwave heating are 0.3% for 000#, 0.6% for 0# and 0.9%-1.1% for 2#. Considering the volumetric properties of the asphalt mixture, it is not recommended that the content of 2# fiber exceeds 0.9%. As for the type of steel wool, the addition of 2# steel wool can provide the highest surface temperature though it required the highest optimal steel wool content (0.9% - 1.1%) compared with 000# (0.3%) and 0# (0.6%). On the other hand, the 000# has the lowest MH improvement due to the fact that only limited amount of steel wool can be used because of the dispersion problem at mixing.

At last, the temperature gap among various irradiation times is not equally distributed, indicating that the temperature raising rate of specimens with different steel wool fiber are different. As shown in Fig.9, the bigger temperature gaps among the irradiation time over the initial, midterm and final stages are marked by the gray background. The average temperature raising rates of mixture with 000# fiber are 1.5 °C/s, 0.7 °C/s and 0.5 °C/s at the moments of 20s, 80s and 140 s respectively; the figure for 0# are 1.4 °C/s, 1.0 °C/s, 0.7 °C/s and 0.6 °C/s at the moments of 20s, 40s, 100s and 160 s respectively; for 2# are 1.5 °C/s, 1.2 °C/s, 0.8 °C/s and 0.6 °C/s at the moments of 20s, 40s, 100s and 160 s respectively. Apparently, the temperature raising rate decreases with increasing the irradiation time though the longer irradiation leads to higher surface temperature.

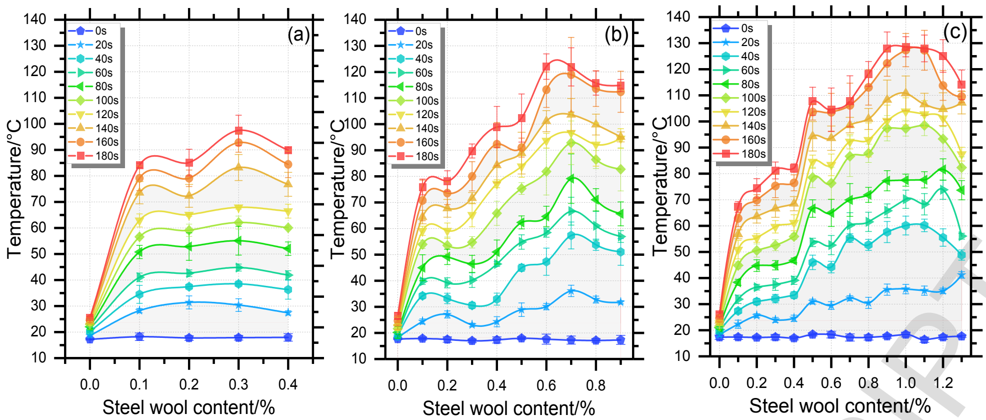

(a) 000# steel wool; (b) 0# steel wool; (c) 2# steel wool

Fig.9 Surface temperature of asphalt mixtures

In winter, the road pavement may experience various low-temperature environments. Therefore, the MH capacities of specimen with initial temperatures of - 5 °C and - 10 °C are tested, the results are presented in Fig. 10. After the calculation of temperature differences in every content at all moments (except for 0% at 0 s), the average temperature difference between the specimens with initial temperature - 5 °C and - 10 °C are 6.9 °C (000#), 6.2 °C (0#) and 1.9 °C (2#), respectively, these figures are close to the initial temperature difference - 5 °C. It indicates that the initial temperature of the specimen can affect the ultimate temperature of the specimen after microwave heating, but the effect becomes less obvious as the irradiation time increases.

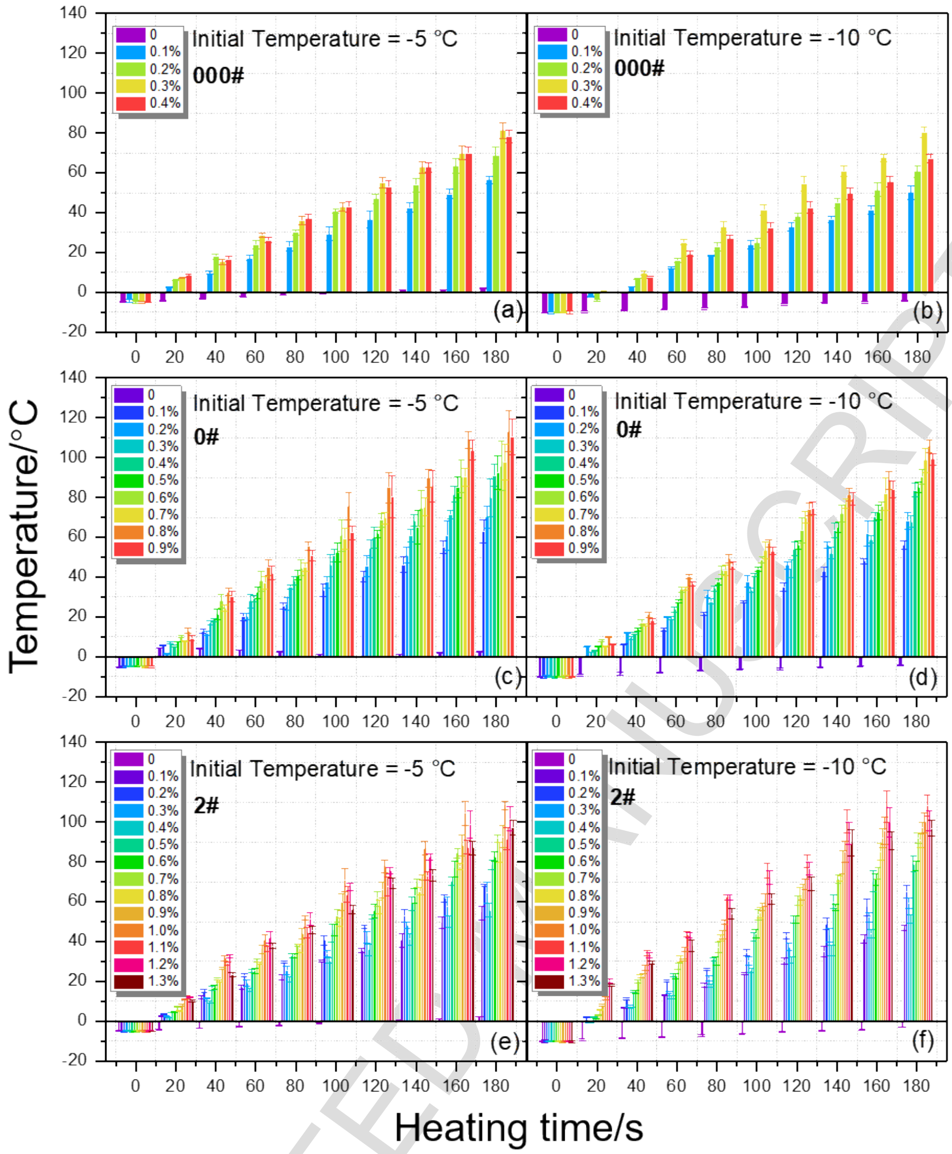

Fig.10 MH profiles of specimens under initial temperature of - 5 °C and - 10 °C

4.3 Ice-thawing time

The ice-thawing time of asphalt specimens prepared with three types of steel wool was determined by the accelerated MH de-icing device under the initial temperatures of - 5 °C and - 10 °C, the results are illustrated in Fig. 11. Firstly, the incorporation of steel wool can significantly enhance the MH ice-thawing efficiency of asphalt mixtures, regardless of initial temperature, type or content of steel wool. For 000# steel wool, the ice-thawing time reaches a minimum of 68 s (- 5 °C) and 92 s (- 10 °C) when the steel wool content is 0.3%. Meantime, the specimens containing

0 # steel wool had the ice thawing time decrease with the increase of steel wool content up to 0.7%, and then the ice thawing time increases as the content of steel wool increases. Notably, the thawing time of specimens with 0.4% - 0.7% 0# steel wool stay in a close range of 57 s to 66 s (- 5 °C) and 65 s to 72 s (- 10 °C). When the 2# steel wool was used, the ice-thawing time is dramatically shortened from 266 s and 292 s for initial temperature of -5 °C and -10 °C, respectively, to just 38 s and 53 s when the steel wool contents reaches 1.0%, then a significant increase of ice-thawing time is observed as the steel wool contents increases. As a result, the MH ice-thawing efficiency can reach the maximum when 1.0% of 2# steel wool was used in asphalt mixture.

In addition, the average ice-thawing time for specimens without steel wool is 266 s and 292 s at initial temperature of - 5 °C and - 10 °C, respectively. According to above, the optimal steel wool contents in specimens for the highest ice-thawing efficiency are 0.3% of 000#, 0.7% of 0# and 1.0% of 2# steel wool. The MH deicing efficiency of conventional asphalt mixture is improved by 2.9, 3.6 and 6.0 times with initial temperature of - 5 °C, while it is enhanced by 2.1, 3.4 and 4.5 times with initial temperature of - 10 °C. The average ice-thawing time that specimens need under - 10 °C is 9.3% (000#), 11.3% (0#) and 14.8% (2#) longer than that of - 5 °C, indicating that the lower initial temperature is responsible for reduction in the ice-thawing efficiency of MH pavement.

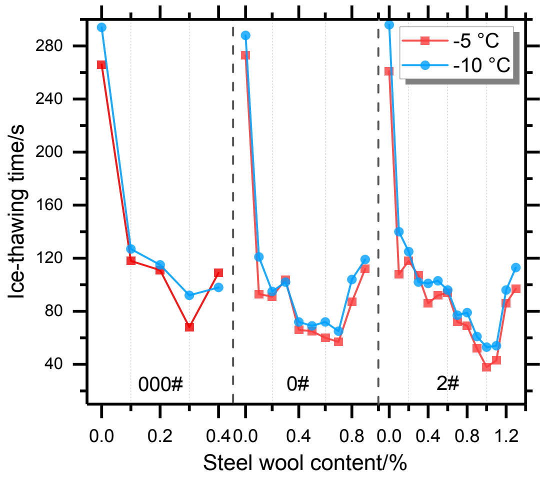

Fig. 11 Ice-thawing time required under initial temperatures of - 5 °C and - 10 °C

The efficiency of snow melting pavement is sensitive to the thickness of ice layer covered on pavement. (Xu et al., 2018). To evaluate the effect of ice layer thickness on the thawing time of specimens, ice layer thicknesses of 3 cm, 4 cm and 5 cm are selected, to assess the thawing effectiveness under extremely adverse environmental conditions, the results are shown in Fig. 12. The average ice-thawing time of specimens covered with 4 cm ice layer is 3.2% (000#), 10.8% (0#) and 14.1% (2#) longer than that of 3 cm ice layer; while 5 cm ice layer demands 8.6% (000#), 4.7% (0#), and 11.8% (2#) longer ice-thawing time compared to that of 4 cm. Approximately, every 1cm increase in ice layer thickness demands 5.9% (000#), 7.7% (0#) and 13.0% (2#) increase in heating time when the ice thickness between 3cm and 5cm. Therefore, the increase in ice layer thickness can only results in a slight growth in the ice-thawing time of MH pavement containing steel wool, even when the ice layer is up to 5cm thick. This is due to the limited dielectric loss tangent of the ice (0.0009 at 12 °C) which is proportional to the heat absorbing capacity of materials (Thomson et al., 2013). Therefore, the electromagnetic energy is hardly attenuated when penetrating the ice layer. This characteristic enables the pavement MH deicing technology to be potentially used to help those regions with harsh road environment caused by severe freezing climate. The effect of steel wool content on the ice-thawing time of specimens under various ice layer thicknesses shows a similar trend, the incorporation of steel wool fiber shortens the ice-thawing time effectively when the steel wool fiber contents are lower than a certain amount, then the ice-thawing requires more radiation duration when the fiber contents exceed the optimal amount regardless the fiber type and ice layer thickness. This phenomenon is resulted from the difference in microwave heating capacity of specimens containing various fiber contents.

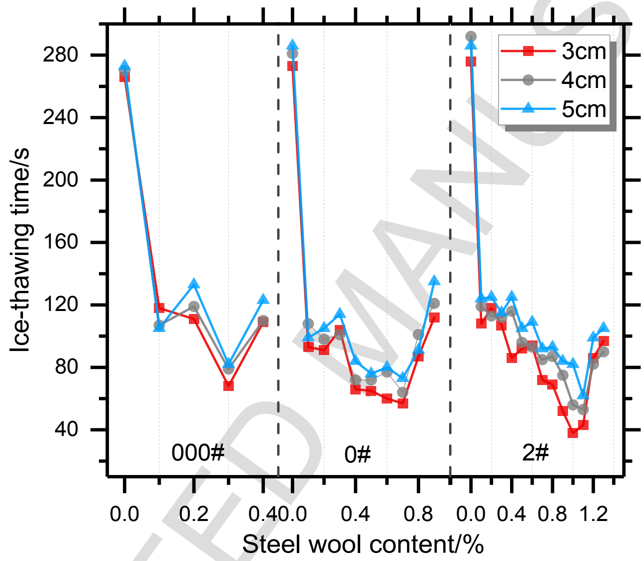

Fig. 12 Ice-thawing time required by specimen covered with various thickness of ice layers

4.4 Microwave heating uniformity

As an anisotropic and non-homogeneous material, the pavement presents a temperature field that tends to be unevenly distributed due to the difference in microwave absorption of the specimen surface (Sun et al., 2017). In practice, the ice layer may be difficult to be completely removed by the microwave heating since the interface adhesion remains strong where the pavement has lower microwave absorption. Fig. 13 presents the temperature distribution of the specimens with the 000# (0.3%), 0# (0.7%) and 2# (0.9%) steel wool at the initial stage (20 s), midterm stage (100 s) and final stage (180 s) of the microwave heating process, respectively. It can be seen that the multiple temperature peaks are distributed across various positions of the specimen surface, supporting the fact that the surface temperature is not uniform at any heating stages. In addition, the standard deviation of the temperature field reflects its distribution uniformity while the temperature range describes the temperature difference of the field. In Fig. 13, both the temperature range and standard deviation stay at a limited level at the initial heating stage (20 s), indicating a desirable uniformity. When the heating process reaches the midterm stage (100 s), the temperature standard deviations of 000#, 0# and 2# specimens increase by 1.9, 4.4 and 4.6 times than initial stage while the temperature ranges increase by 1.3, 5.5 and 3.6 times, respectively. At last, the difference is even more pronounced when the heating time reaches the final stage. Above phenomenon can be explained as followings. When microwave heating starts, the areas with the desirable fiber concentration (the temperature peaks shown in temperature field) raise sharply while the areas with the poor heating performance grew slowly. As heating continues, the temperature gap among areas expanded because the rate of heat accumulation in each area is different. In summary, results shown in Fig. 13 support the fact that the specimens' heating uniformity significantly decrease as the heating process continues regardless of the steel wool contents or types. The heating uniformity is a key concern if the MH pavement is introduced in the practical use. During microwave deicing, the ice layer covered on the area with lower heating capacity may remain a considerable adhesion with pavement after the microwave heating, thereby it has a potential risk to see the residual ice layer distributed on the MH pavement. Therefore, the heating uniformity should be quantitatively evaluated in the MH pavement design.

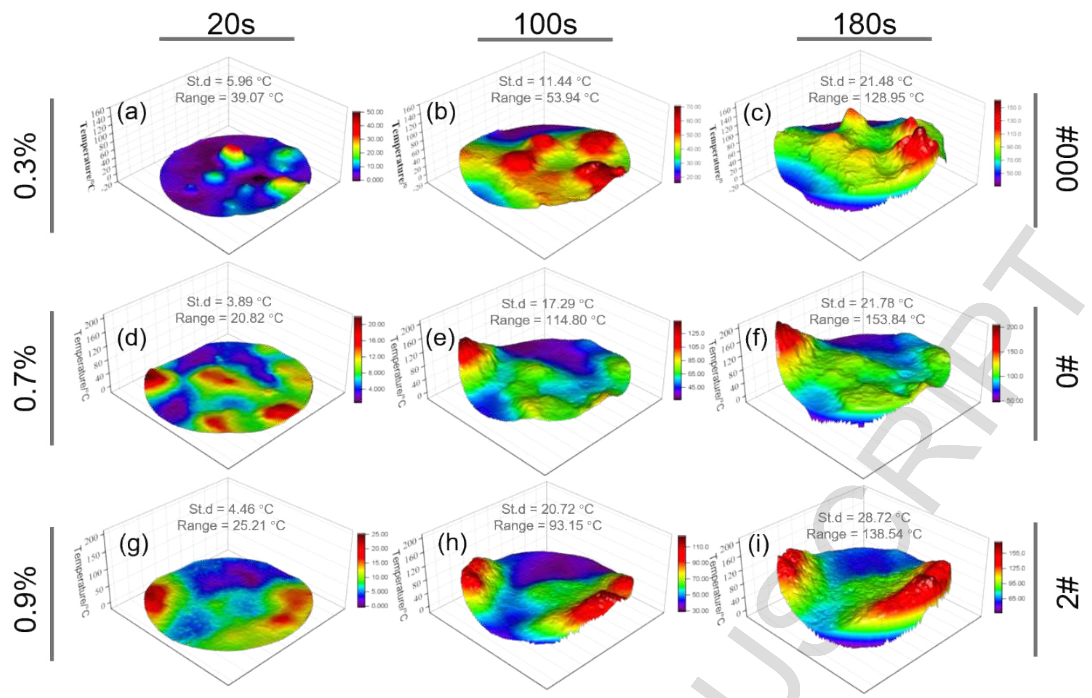

Fig. 13 Surface temperature distribution

The heating uniformity of specimens with various steel wool types and contents are tested and represented by standard deviations in which higher standard deviations indicate less heating uniformity, the results are demonstrated in Fig. 14. The temperature standard deviations of 000#, 0# and 2# specimens are in good correlation with their steel wool contents. Besides, the heating uniformity of specimens deteriorates as the steel wool contents increase regardless of the steel wool types. Meantime, the incorporation of 2# steel wool contributes to a better heating uniformity compared to that of 000# and 0# under the same steel wool content. This indicates that increase the diameter of the steel wool helps to improve the heating uniformity of asphalt mixture.

Furthermore, the temperature peak shown in Fig. 13 indicates a position at which overheating may occur. Generally, such overheating may change the rheological and mechanical performances of asphalt concrete. However, the pavement covered with ice layer under the low ambient temperature may not suffer this problem because the heat generated by steel wool fiber will be transferred to the mixture and ice layer synchronously and continuously, resulting to a lower surface temperature.

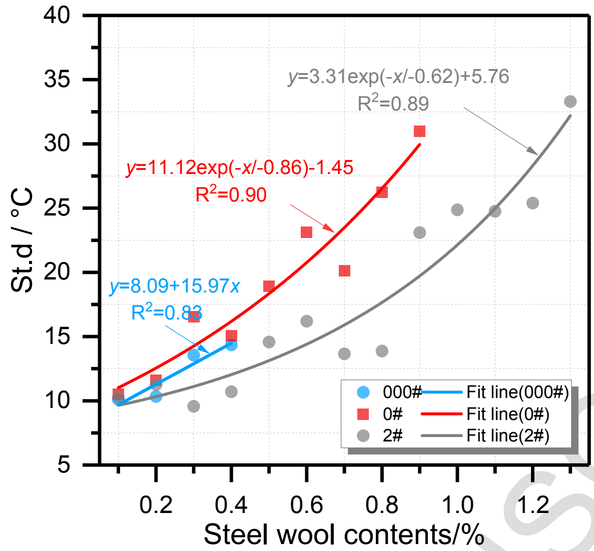

Fig. 14 Standard deviations of surface temperature field

4.5 Durability of heating capacity

The number of cycles times was determined based on historical data (2011 - 2018) of the average number of days in a year that snowfall or rainfall occurred when air temperature was below 0 °C. Data of five cities typical in north China were obtained, the results are 10.3, 7.0, 14.1, 11.5 and 20.9 days for Beijing, Xi'an, Ordos, Datong and Harbin, respectively (Tianqi, 2018). On average, the MH pavement may experience approximately 13 freeze-thaw cycles in a winter based on the assumption that each snowfall at this temperature would cause an ice layer to form on the road surface. The specimens with 0.3% (000#), 0.7% (0#) and 0.9% (2#) steel wool were selected as typical examples, their MH surface temperature over 6 years of freeze-thaw cycles were tested, the results are shown in Fig. 15. It can be seen that the MH capacity of specimens show insignificant degradation with an increase of the cycle times. The analysis of variance (ANOVA) results also proved that there is no statistical significance between cycle times and MH surface temperature.

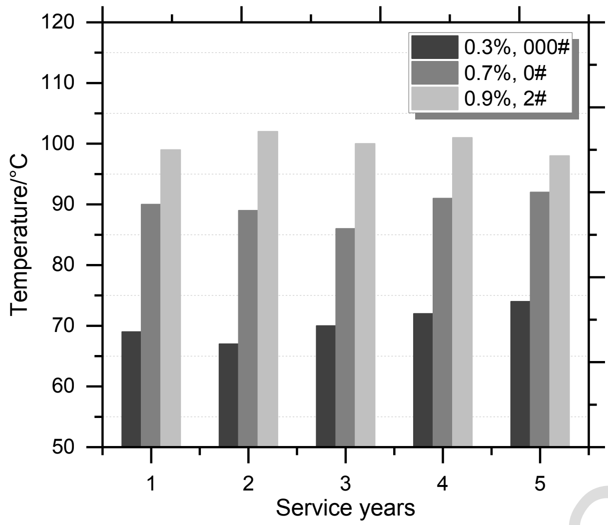

Fig. 15 Surface temperature of specimens after freeze-thaw cycles

It is well-acknowledged that the S434 stainless steel, which is used for manufacturing the steel wool in this study, has stable chemical properties under normal circumstances in terms of temperature, humidity and chemistry. This material characteristic offers a stability and electromagnetic performance to asphalt mixtures containing the steel wool under repeated service cycles in winter. On the other hand, previous studies indicated that the corrosion process of steel wool or steel fiber can be accelerated under coastal atmospheric environment (NaCl) and acidic rain ($NaHSO_3$) (Marcos-Meson et al., 2018). Considering that the steel wool is wrapped in the asphalt mortar which can effectively isolates the steel wool from the outside chemical atmosphere, we assume that the steel wool asphalt mixture is durable under adverse conditions. However, this assumption needs to be verified by further test.

5 Conclusion and Recommendation

5.1 Conclusions

This paper aims investigate the feasibility of microwave heating for asphalt mixture containing steel wool. This study contrites to existing body of knowledge by revealing the potential use of steel wool in microwave deicing of asphalt pavements and developing laboratory settings for ice layer preparation, microwave heating and deicing of the asphalt mixture. Based on the results discussed above, the following conclusions can be drawn:

- The increasing steel wool fiber contents lead to the increase of the air void content of asphalt mixture; thicker fibers are recommended for asphalt mixture because it results in lower air void content than thinner fibers. The optimal steel wool contents for asphalt mixtures for microwave heating are 0.3% for 000#, 0.6% for 0# and 0.9% for 2#.
- The lower initial temperature is responsible for reducing the ice-thawing efficiency of MH pavement, the ice layer thickness has limited influence on the ice-thawing efficiency.
- The heating uniformity of specimens deteriorates as the steel wool contents increase regardless the steel wool types. Increasing the diameter of the steel wool helps to improve the heating uniformity of asphalt mixture.

5.2 Further study

This study has verified the feasibility of using steel wool to improve the microwave heating performance of conventional asphalt mixtures for deicing the pavement in winter. The aforementioned conclusions are believed to be reliable though attention should be paid to several issues in the future. Although the specimens' durability of microwave heating capacity was evaluated, the effect of repeated heating on the mechanical properties of asphalt mixtures should be further studied to verify its degradation. In addition, large-scale filed deicing test is recommended to be carried out to verify the laboratory test results, and deal with practical issues in implementing such device for winter road maintenance. At last, the correlation between fiber distribution on microwave heating rate should be further studied as well as the fiber percolation.

Acknowledgement

This work was supported by the China-UK Research and Innovation Partnership Fund (Newton Fund) jointly funded by the China Scholarship Council and British Council, State Key Laboratory of High Performance Civil Engineering Materials（No. 2018CEM010), National and Local Joint Engineering Materials Laboratory of Traffic Engineering and Civil Engineering, Chongqing Jiaotong University (No. LHSYS-2016-002), the Fundamental Research Funds for the Central Universities of China (No. 300102318402), Scientific Project of Henan Provincial Communications Planning & Design Institute Co., Ltd (No. 220231180007), the Project of Key Laboratory for Special Region Highway Engineering of Ministry of Education (Grant No.300102218508). The author would like to thank the pioneering research conducted by previous scholars as well as the constructive comments of reviewers.

References

Bardal, K.G., Jørgensen, F., 2017. Valuing the risk and social costs of road traffic accidents – Seasonal variation and the significance of delay costs. Transport Policy 57, 10-19.

Gao, J., Sha, A., Wang, Z., Tong, Z., Liu, Z., 2017. Utilization of steel slag as aggregate in asphalt mixtures for microwave deicing. Journal of Cleaner Production 152, 429-442.

Gao, J., Zhang, Z., Han, Z., Sha, A., Wang, Z., Jiang, W., 2016. A review of electromagnetic wave absorbing materials used in microwave deicing pavement. Materials Review 30(12), 87-95.

Gao, Z., Jiao, S., Xu, X., Tang, X., 2009. Simulation study on the influence of waveguide end distance to microwave heating efficiency. Journal of Xi'an University of Architecture and Technology 41(3), 371-374.

García, A., Norambuena-Contreras, J., Partl, M.N., 2013. A parametric study on the influence of steel wool fibers in dense asphalt concrete. Materials and Structures 47(9), 1559-1571.

García, Á., Schlangen, E., van de Ven, M., Liu, Q., 2012. A simple model to define induction heating in asphalt mastic. Construction and Building Materials 31, 38-46.

García, Á., Schlangen, E., van de Ven, M., van Vliet, D., 2010. Induction heating of mastic containing conductive fibers and fillers. Materials and Structures 44(2), 499-508.

He, L., Zhao, l., Liu, T., Ma, Y., 2017. Research on induction heating activated self-healing of cracks in dense graded asphalt mixture. China Journal of Highway and Transport 30(1), 17-24.

Hopstock, D.M., Zanko, L.M., 2005. Minnesota taconite as a microwave-absorbing road aggregate material for deicing and pothole patching applications, Final report ed. University of Minnesota Duluth.

Jahanbakhsh, H., Karimi, M.M., Jahangiri, B., Nejad, F.M., 2018. Induction heating and healing of carbon black modified asphalt concrete under microwave radiation. Construction and Building Materials 174, 656-666.

Jardin, E., Uhring, J., Rey, P.B., Ferrier, M., Obert, L., 2014. Snowblower injuries to the hand. Chir Main 33(4), 272-278.

Jiao, S., Tang, X., Gao, Z., Wang, Q., 2008. Study of key technology on microwave deicing efficiency. China Journal of Highway and Transport 21(6), 122-126.

JTGE42-2005, 2005. Testing Procedures of Aggregate for Highway Engineering. Inspection and Quarantine of the People's republic of China, Beijing.

JTGF40-2004, 2004. Technical Specification for Construction of Highway Asphalt Pavement. Inspection and Quarantine of the People’s Republic of China, Beijing.

Karimi, M.M., Jahanbakhsh, H., Jahangiri, B., Moghadas Nejad, F., 2018. Induced heating-healing characterization of activated carbon modified asphalt concrete under microwave radiation. Construction and Building Materials 178, 254-271.

Khaleghei Ghosheh Balagh, A., Naderkhani, F., Makis, V., 2014. Highway Accident Modeling and Forecasting in Winter. Transportation Research Part A: Policy and Practice 59, 384-396.

Li, X., Xu, Y., Lu, F., 2003. Application of microwave heating for ice removal on streets. Journal of Harbin Institute of Technology 35(11), 1342-1343.

Liu, Q., Schlangen, E., García, Á., van de Ven, M., 2010. Induction heating of electrically conductive porous asphalt concrete. Construction and Building Materials 24(7), 1207-1213.

Liu, Q., Schlangen, E., van de Ven, M., 2013. Induction Healing of Porous Asphalt Concrete Beams on an Elastic Foundation. Journal of Materials in Civil Engineering 25(7), 880-885.

Liu, Q., Yu, W., Schlangen, E., van Bochove, G., 2014. Unravelling porous asphalt concrete with induction heating. Construction and Building Materials 71, 152-157.

Liu, Z., Sha, A., He, R., Xing, M., 2016. Antifreeze asphalt mixtures design and antifreeze performances prediction based on the phase equilibrium of natural solution. Cold Regions Science and Technology 129, 104-113.

Marcos-Meson, V., Michel, A., Solgaard, A., Fischer, G., Edvardsen, C., Skovhus, T.L., 2018. Corrosion resistance of steel fibre reinforced concrete - A literature review. Cement and Concrete Research 103, 1-20.

Menozzi, A., Garcia, A., Partl, M.N., Tebaldi, G., Schuetz, P., 2015. Induction healing of fatigue damage in asphalt test samples. Construction and Building Materials 74, 162-168.

Norambuena-Contreras, J., Garcia, A., 2016. Self-healing of asphalt mixture by microwave and induction heating. Materials & Design 106, 404-414.

Obaidi, H., Gomez-Meijide, B., Garcia, A., 2017. A fast pothole repair method using asphalt tiles and induction heating. Construction and Building Materials 131, 592-599.

Osborne, T.L., Hutcheson, W.R., 1987. Asphalt compounds and method for asphalt reconditioning using microwave radiation. The Titan Corporation, Valparaiso, Ind., United States.

Pan, P., Wu, S., Xiao, Y., Liu, G., 2015. A review on hydronic asphalt pavement for energy harvesting and snow melting. Renewable and Sustainable Energy Reviews 48, 624-634.

Park, P., El-Tawil, S., Park, S.-Y., Naaman, A.E., 2015. Cracking resistance of fiber reinforced asphalt concrete at −20°C. Construction and Building Materials 81, 47-57.

Rivett, M.O., Cuthbert, M.O., Gamble, R., Connon, L.E., Pearson, A., Shepley, M.G., Davis, J., 2016. Highway deicing salt dynamic runoff to surface water and subsequent infiltration to groundwater during severe UK winters. Sci Total Environ 565, 324-338.

Strong, C.K., Ye, Z., Shi, X., 2010. Safety Effects of Winter Weather: The State of Knowledge and Remaining Challenges. Transport Reviews 30(6), 677-699.

Sun, Y., 2013. Design and research of parts and walk synchronization system of the vehicle for snow and ice removing based on microwave heating, School of Mechanical Engineering. Yanshan University, Qinhuangdao, China.

Sun, Y., Wu, S., Liu, Q., Hu, J., Yuan, Y., Ye, Q., 2018. Snow and ice melting properties of self-healing asphalt mixtures with induction heating and microwave heating. Applied Thermal Engineering 129, 871-883.

Sun, Y., Wu, S., Liu, Q., Zeng, W., Chen, Z., Ye, Q., Pan, P., 2017. Self-healing performance of asphalt mixtures through heating fibers or aggregate. Construction and Building Materials 150, 673-680.

Tang, X., 2009. Study of microwave deicing efficiency on road, School of Mechanical Engineering. Chang'an University, Xi'an, China.

Tang, Z., Hong, T., Liao, Y., Chen, F., Ye, J., Zhu, H., Huang, K., 2018. Frequency-selected method to improve microwave heating performance. Applied Thermal Engineering 131, 642-648.

Theofilatos, A., 2017. Incorporating real-time traffic and weather data to explore road accident likelihood and severity in urban arterials. J Safety Res 61, 9-21.

Thomson, L.I., Osinski, G.R., Pollard, W.H., 2013. Application of the Brewster angle to quantify the dielectric properties of ground ice formations. Journal of Applied Geophysics 99, 12-17.

Tianqi, 2018. Historical climate data of China. http://lishi.tianqi.com/. (Accessed 24/2/2018 2018).

Usman, T., Fu, L., Miranda-Moreno, L.F., 2010. Quantifying safety benefit of winter road maintenance: accident frequency modeling. Accid Anal Prev 42(6), 1878-1887.

Wang, H., Yang, J., Liao, H., Chen, X., 2016. Electrical and mechanical properties of asphalt concrete containing conductive fibers and fillers. Construction and Building Materials 122, 184-190.

Wang, Z., Gao, J., Ai, T., Zhao, P., 2014. Laboratory Investigation on Microwave Deicing Function of Micro Surfacing Asphalt Mixtures Reinforced by Carbon Fiber. Journal of Testing and Evaluation 42(2), 20130118.

Wang, Z., Wang, H., An, D., Ai, T., Zhao, P., 2016a. Laboratory investigation on deicing characteristics of asphalt mixtures using magnetite aggregate as microwave-absorbing materials. Construction and Building Materials 124, 589-597.

Wang, Z., Xu, C., Wang, S., Gao, J., Ai, T., 2016b. Utilization of magnetite tailings as aggregates in asphalt mixtures. Construction and Building Materials 114, 392-399.

Wang, Z., Zhang, T., Zhou, L., 2016c. Investigation on electromagnetic and microwave absorption properties of copper slag-filled cement mortar. Cement and Concrete Composites 74, 174-181.

Wyman, D.A., Koretsky, C.M., 2018. Effects of road salt deicers on an urban groundwater-fed kettle lake. Applied Geochemistry 89, 265-272.

Xu, H., Wang, D., Tan, Y., Zhou, J., Oeser, M., 2018. Investigation of design alternatives for hydronic snow melting pavement systems in China. Journal of Cleaner Production 170, 1413-1422.

Ye, Z., Shi, X., Strong, C.K., Larson, R.E., 2012. Vehicle-based sensor technologies for winter highway operations. IET Intelligent Transport Systems 6(3), 336.

Yu, W., Li, S., Wenjie, F., Yi, X., 2011. Snow and ice melting techniques of pavement: state of the art and development tendency. Journal of Glaciology and Geocryology 33(4), 933-940.

Zítková, J., Hegrová, J., Anděl, P., 2018. Bioindication of road salting impact on Norway spruce (

Picea abies). Transportation Research Part D: Transport and Environment 59, 58-67.

Zhang, Q., Yu, Y., Chen, W., Chen, T., Zhou, Y., Li, H., 2016. Outdoor experiment of flexible sandwiched graphite-PET sheets based self-snow-thawing pavement. Cold Regions Science and Technology 122, 10-17.

Zhou, Z., Wang, X., Zhang, X., Chen, G., Zuo, J., Pullen, S., 2015. Effectiveness of pavement-solar energy system – An experimental study. Applied Energy 138, 1-10.

Highlights

i) A novel use of microwave heating is introduced for icy pavement deicing;

ii) Laboratory set up of microwave heating, thawing test for asphalt mixture are designed;

iii) Microwave ice-thawing performances of asphalt mixture with steel fibers are tested;

and iv) Optimal steel fiber contents were recommended for microwave deicing pavement.